



This open access document is posted as a preprint in the Beilstein Archives at <https://doi.org/10.3762/bxiv.2021.91.v1> and is considered to be an early communication for feedback before peer review. Before citing this document, please check if a final, peer-reviewed version has been published.

This document is not formatted, has not undergone copyediting or typesetting, and may contain errors, unsubstantiated scientific claims or preliminary data.

Preprint Title	Stimuli-responsive polypeptide nanogels loaded with α 1-antitrypsin for inhibition of inflammatory mediator trypsin
Authors	Petr Šálek, Jana Dvořáková, Sviatoslav Hladysh, Diana Oleshchuk, Ewa Pavlova, Jan Kučka and Vladimír Proks
Publication Date	23 Dez. 2021
Article Type	Full Research Paper
ORCID® IDs	Petr Šálek - https://orcid.org/0000-0002-5021-9794 ; Ewa Pavlova - https://orcid.org/0000-0002-6693-9040 ; Jan Kučka - https://orcid.org/0000-0003-2489-5315 ; Vladimír Proks - https://orcid.org/0000-0001-7368-7120

License and Terms: This document is copyright 2021 the Author(s); licensee Beilstein-Institut.

This is an open access work under the terms of the Creative Commons Attribution License (<https://creativecommons.org/licenses/by/4.0>). Please note that the reuse, redistribution and reproduction in particular requires that the author(s) and source are credited and that individual graphics may be subject to special legal provisions.

The license is subject to the Beilstein Archives terms and conditions: <https://www.beilstein-archives.org/xiv/terms>.

The definitive version of this work can be found at <https://doi.org/10.3762/bxiv.2021.91.v1>

Stimuli-responsive polypeptide nanogels loaded with α 1-antitrypsin for inhibition of inflammatory mediator trypsin

Petr Šálek ^{1*}, Jana Dvořáková ¹, Sviatoslav Hladysz ¹, Diana Oleshchuk ^{1,2}, Ewa Pavlova ¹, Jan Kučka ¹, Vladimír Proks ¹

¹ Institute of Macromolecular Chemistry, Academy of Sciences of the Czech Republic, Heyrovského nám. 2, 162 06 Prague 6, Czech Republic

² Department of Physical and Macromolecular Chemistry, Faculty of Science, Charles University, Hlavova 8, 128 40 Prague 2, Czech Republic

* Corresponding author: salek@imc.cas.cz; Tel.: +420 296 809 225

Abstract: A new type of hydrophilic, biocompatible, and biodegradable polypeptide nanogel depots loaded with natural serine protease inhibitor α 1-antitrypsin (AAT) was applied for inhibition of inflammatory mediator trypsin. Further, poly[*N*⁵-(2-hydroxyethyl)-L-glutamine-*ran*-*N*⁵-propargyl-L-glutamine-*ran*-*N*⁵-(6-aminoethyl)-L-glutamine]-*ran*-*N*⁵-[2-(4-hydroxyphenyl)ethyl]-L-glutamine] (PHEG-Tyr) and *N* α -L-Lysine-grafted α,β -poly[(2-propyne)-DL-aspartamide-*ran*-(2-hydroxyethyl)-DL-aspartamide-*ran*-(2-(4-hydroxyphenyl)ethyl)-DL-aspartamide] (*N* α -Lys-NG) nanogels were prepared by HRP/H₂O₂-mediated crosslinking in inverse miniemulsions with pH and temperature-stimuli responsive behavior confirmed by dynamic light scattering and zeta potential measurements. The loading capacity of PHEG-Tyr and *N* α -Lys-NG nanogels and their release profiles were firstly optimized with bovine serum albumin (BSA) and then used for loading and release of AAT. PHEG-Tyr and *N* α -Lys-NG nanogels showed different loading capacities for AAT with the maximum (20 %) achieved with *N* α -Lys-NG nanogel. In both cases, the nanogels depots demonstrated a burst release of AAT during 6 h, which could be favorable for quick inhibition of trypsin. A consequent pilot *in vitro* inhibition study revealed that both PHEG-Tyr and *N* α -Lys-NG nanogels loaded with AAT successfully inhibited the enzymatic activity of trypsin. Furthermore, the inhibitory efficiency of the AAT-loaded

nanogels was higher than that of AAT itself, indicating that the negatively charged polypeptide nanogels enhance the inhibitory function of AAT loaded in the nanogel depots.

Keywords: α_1 -antitrypsin, inflammatory mediator, nanogel, polypeptide, trypsin

Introduction

Despite significant and progressive advances in medicine, a global incidence of pancreatitis shows that this disease remains one of the most severe health problems [1]. Pancreatitis is an inflammatory disease of the pancreas categorized as either acute pancreatitis, which occurs suddenly as a short-term illness, or chronic pancreatitis, which is a long-lasting condition. Acute pancreatitis may lead to chronic pancreatitis with a high risk of consecutive development of cancer [2,3]. The pancreas has exocrine and endocrine functions where the exocrine serves to secrete digestive enzymes, such as trypsin, into the intestine. Trypsin belongs to a group of serine proteases and is excreted by the pancreas in an inactive form known as trypsinogen with subsequent activation in the duodenum. However, premature activation of trypsinogen in pancreatic acinar cells starts the inflammatory process in which trypsin induces proteolysis, pancreatic injury, and the onset of pancreatitis [4,5].

Various organisms naturally produce inhibitors of serine proteases to regulate their inappropriate proteolytic activity which may lead to undesirable inflammatory processes [6]. Beneficial biological activity of serine protease inhibitors has been successfully exploited for therapeutic purposes or antinutritional properties [7,8]. Different types of small proteins or polypeptides represent a class of bioactive compounds identified as inhibitors of serine proteases. Aprotinin, a Kunitz type serine protease inhibitor, is well known for its trypsin inhibitory activity [9]. Other examples are ulinastatin, a glycoprotein found in urine, plasma, and all organs, and gabexate, a synthetic serine protease inhibitor that inhibits secretion and activity of trypsin. Both are successfully used for the treatment of acute pancreatitis [10]. The pancreas itself secretes the serine protease inhibitor Kazal type 1 (SPINK1) to inhibit trypsinogen autoactivation and proteolytic activity of trypsin. A loss in SPINK1 secretion and function increases the risk of pancreatitis development [4]. As a defense mechanism against serine proteases and other inflammatory mediators, organisms secrete many other serine proteases inhibitors, such as α_1 -antitrypsin (AAT), α_2 -macroglobulin, α_1 -antichymotrypsin, eglin C, etc [11]. However, direct intravenous or oral administration of the majority of these natural serine protease inhibitors is ineffective due to their low plasma and peritoneal levels, very short in-vivo half-lives, chemical instability, and high susceptibility to degradation [6].

Delivery systems represented by various polymer particles provide necessary and effective protection for a bioactive cargo against degradation and elimination as well as for prolonged circulation time. Nanogels, soft hydrogel nanoparticles, have been proved efficient carriers of proteins or peptides preserving the biological activity of their payload [12-14]. For instance, Ozawa et al. introduced nanogel from highly branched cyclic dextrin derivatives which trapped fluorescein isothiocyanate-labeled insulin that was continuously released over 12 hours [15]. Hirakura et al. fabricated cholesteryl group-bearing pullulan nanogel serving as a reservoir of three various proteins, glucagon-like peptide 1, insulin and erythropoietin incorporated in hyaluronan hydrogel [16]. Morimoto et al. prepared acid-labile cholesteryl-modified pullulan nanogel which complexed with loaded bovine serum albumin and released it under acidic conditions [17]. Landfester et al. used a bio-orthogonal reaction to fabricate the dextran nanogel with pH-responsive hydrazine linkages allowing a controlled release of loaded FITC-albumin [18]. With regard to inhibition of serine proteases and inflammation, AAT, the most abundant inhibitor of serine proteases in human plasma, regulates the proteolytic activity of secreted proteases and is involved in acute anti-inflammatory response against inflammatory mediators [19]. Interestingly, it was revealed that subjects with AAT deficiency had increased activation of neutrophils, levels of cytokines, and inflammation, and that AAT administration slowed down a decrease in insulin production during diabetes [20,21]. A few poly (D,L-lactide-co-glycolide) nanoparticles loaded with AAT were successfully manufactured and AAT release profiles from the nanoparticles were investigated [21,22].

In this work, we have designed two types of nanogels from biocompatible and biodegradable PHEG-Tyr and biocompatible and non-biodegradable N_α -Lys-NG polypeptide precursors by HRP/H₂O₂-mediated crosslinking in inverse miniemulsion for delivery of AAT for inhibition of inflammatory mediator. Both prepared polypeptide nanogels demonstrate stimuli-responsive behavior under different pH and temperatures. After optimizing the loading and release from PHEG-Tyr and N_α -Lys-NG with BSA, the AAT loading and release were investigated. The results show that AAT has a higher affinity to N_α -Lys-NG and both nanogel depots demonstrate burst release over 6 h followed by continuous release over ~ 160 h. Finally, the PHEG-Tyr and N_α -Lys-NG nanogels loaded with AAT were successfully applied for pilot *in vitro* inhibition studies of trypsin activity.

Results and Discussion

Preparation of polyglutamine (PHEG-Tyr) and zwitterionic polyaspartamide (N_{α} -Lys-NG) nanogels

Synthetic polypeptides PHEG-Tyr and N_{α} -Lys-NG, which were prepared and characterized according to earlier published procedures [23,25], were nanogelated in inverse miniemulsion via HRP/H₂O₂ crosslinking approach to obtain the chemically dityramine-crosslinked nanogels [23]. Additionally, our previous studies presented *in vitro* and *in vivo* tests documenting biocompatibility and biodegradability of PHEG-Tyr nanogel and biocompatibility of N_{α} -Lys-NG nanogel [23-25]. In this study, we have optimized the preparation of biocompatible and biodegradable PHEG-Tyr nanogel by mixing SPAN 80 surfactant with TWEEN 85 where combining these surfactants leads to the formation of PHEG-Tyr nanogel with a more spherical shape (Figure 1a) [24]. TEM microscopy analysis has revealed a slight narrowing of particle size distribution with $D = 1.43$. The PHEG-Tyr nanogel is composed of two families of compact hydrogel spheres with $D_n = 111$ nm and 19 nm, and $D_w = 159$ nm and 24 nm, respectively. Biocompatible zwitterionic N_{α} -Lys-NG was synthesized according to our earlier study [25] and TEM image analysis of N_{α} -Lys-NG has demonstrated that the nanogel are more irregular in shape and collapse in the dry state (Figure 1b). This can be the result of the softer structure of N_{α} -Lys-NG nanogel with D_n from 50 to 180 nm.

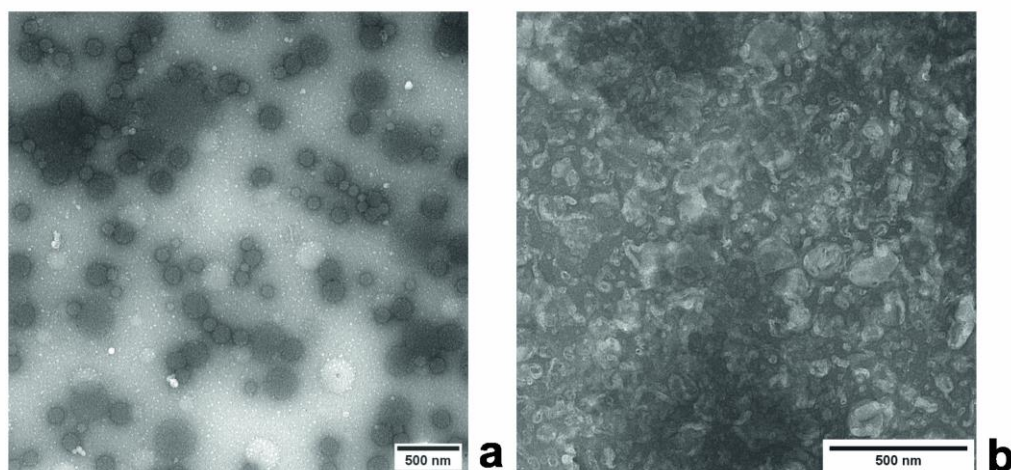


Figure 1. TEM images of PHEG-Tyr (a) and N_{α} -Lys-NG (b) nanogels prepared by HRP/H₂O₂-mediated crosslinking in inverse miniemulsion.

Stimuli-responsive behavior of PHEG-Tyr and N_{α} -Lys-NG nanogels

As the formed polypeptides are polyelectrolytes, their stimuli responsive behavior was studied [26]. Here, biocompatible and biodegradable PHEG-Tyr and biocompatible N_α -Lys-NG were incubated at different pHs and temperatures to study their physicochemical properties represented by D_H and zeta potential. Figure 2a depicts the change in D_H of PHEG-Tyr nanogel as a response to pH variation from 4 to 4.7 at 25 °C, showing a continuous increase of D_H from 179 nm to 205 nm as a result of the protonation of amine groups of PHEG-Tyr nanogel and expansion of PHEG-Tyr nanogel network state due to predominant polymer-medium interaction [27]. With the subsequent increase of pH to 7.4, D_H of PHEG-Tyr nanogel started to decrease to 131 nm, probably due to its collapse and shrinkage. The same trend was observed for the measurement of pH-stimuli responsive behavior of D_H of the PHEG-Tyr nanogel at 37 °C (Figure 2a). Interestingly, DLS measurements reveal a thermal transition of the PHEG-Tyr nanogel with significantly smaller D_H ; about 30-40 nm at 37 °C. This observation indicates that PHEG-Tyr nanogel was more solubilized at 25 °C, compared to behavior at 37 °C when the polymer-polymer interactions prevailed [28]. Zeta potential of PHEG-Tyr nanogel was measured to determine the surface properties at different pHs and temperatures. Figure 2b shows that the zeta potential of PHEG-Tyr nanogel was not affected by pH change and slightly anionic due to excess of carboxyl end groups and hydroxyl groups [23]. Negligible decrease of zeta potential from ~ 6 mV to ~ 8 mV was observed at 25 °C as compared to behavior at 37 °C, suggesting better colloidal stability and polymer-medium interaction [27].

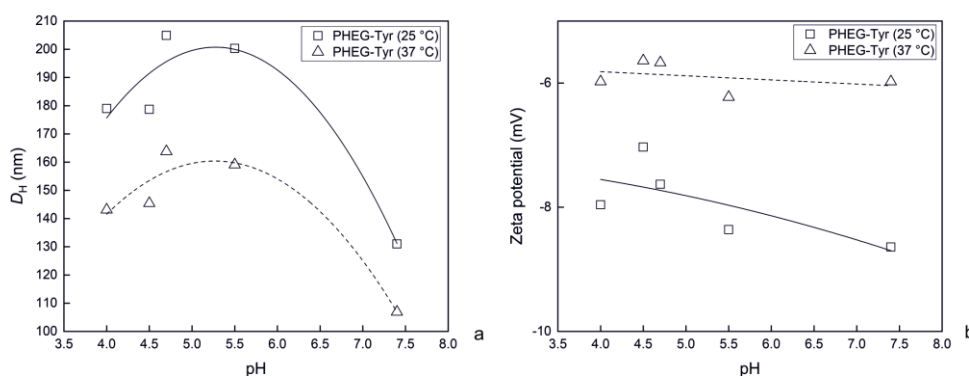


Figure 2. pH dependence of D_H (a) and zeta potential (b) of PHEG-Tyr nanogel at 25 (□) and 37 °C (Δ).

The measurement of the stimuli-responsive properties of N_α -Lys-NG nanogel showed a different behavior compared to PHEG-Tyr nanogel (Figure 3a). The increase of D_H from 200 nm to 240 nm measured at 25 °C was observed when pH was raised from 4 to 7.4. This is ascribed to the expansion of the N_α -Lys-NG nanogel. At 37 °C, the D_H values were also significantly smaller in comparison to the measurement at 25 °C as a result of prevailing hydrophobic interactions. D_H of the N_α -Lys-NG nanogel at 37 °C was also influenced by the change of pH and raised from 190 nm to 215 nm with the increase of pH. The surface charge analysis showed that N_α -Lys-NG nanogel was more anionic in comparison to PHEG-Tyr nanogel due to the presence of carboxyl group of lysine in the side chains of zwitterionic N_α -Lys-NG nanogel [25,29]. The zeta potentials of N_α -Lys-NG nanogel were not significantly affected by the change of temperature (Figure 3b). However, a slight decrease of zeta potential with increasing pH from 4 to 7.4 from approximately -17 mV to -25 mV was observed indicating better colloidal stability of N_α -Lys-NG nanogel at pH 7.4 caused by the fact that the polypeptide chains of N_α -Lys-NG nanogel are more relaxed and expanded. This assumption was also supported by D_H dependence (Figure 3a), showing D_H maximum at pH 7.4.

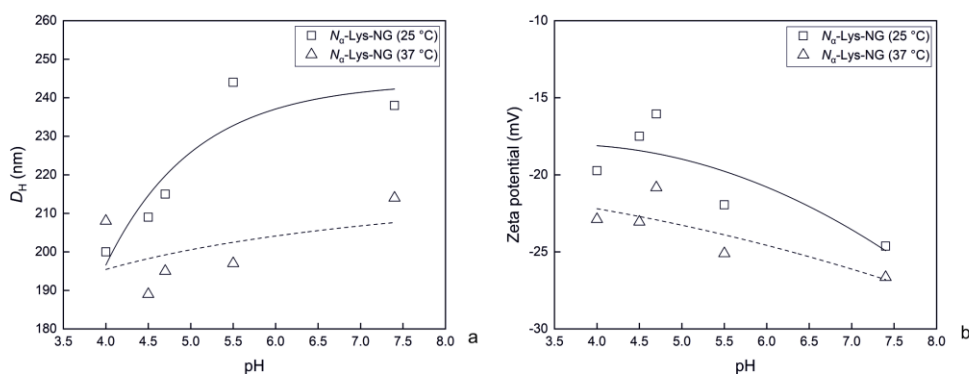


Figure 3. pH dependence of D_H (a) and zeta potential (b) of N_α -Lys-NG nanogel at 25 (□) and 37 °C (Δ).

¹²⁵I-radiolabeling, adsorption and release of bovine serum albumin (BSA) and α -1-antitrypsin (AAT)

Next, the optimization studies of *in vitro* loading of ¹²⁵I-radiolabeled BSA as a model protein and its release from PHEG-Tyr (a) and N_α -Lys-NG nanogels were performed. ¹²⁵I-radiolabeled BSA

was loaded onto PHEG-Tyr nanogel at pH 4.7 and 25 °C because PHEG-Tyr nanogel exhibited the most swollen state and a negative charge at these conditions (Figure 2a and b). The uptake of BSA was found to be more efficient at or below the isoelectric point of BSA (pI 4.7) and, thus, BSA adsorption is driven by the electrostatic and hydrophobic interactions [30,31]. PHEG-Tyr nanogel was incubated with three different ¹²⁵I-radiolabeled BSA concentrations (1, 0.75, and 0.5 mg/ml), and the loading efficiency was found to be low, 2.1 (21 µg/ml), 1.9 (15 µg/ml), and 3.3 % (17 µg/ml), respectively. This could be explained by the weak interaction between ¹²⁵I-radiolabeled BSA and PHEG-Tyr nanogel at pH 4.7 and 25 °C and the low capturing ability of PHEG-Tyr nanogel [32]. As a next step, PHEG-Tyr nanogel loaded with ¹²⁵I-radiolabeled BSA was incubated at pH 7.4 to simulate the physiological environment, and the burst release of ¹²⁵I-radiolabeled BSA from PHEG-Tyr nanogel was observed within 1 h (Figure 4a). The amount of the released ¹²⁵I-radiolabeled BSA was seen to increase with the decrease of initial concentration of ¹²⁵I-radiolabeled BSA during the loading onto PHEG-Tyr nanogel. Furthermore, some amount of ¹²⁵I-radiolabeled BSA was not released and remained entrapped in the PHEG-Tyr nanogel. This was ascribed to the shrinkage of PHEG-Tyr nanogel after the change of pH from 4.7 to 7.4 (Figure 2a).

Next loading experiments showed that ¹²⁵I-radiolabeled BSA had a better affinity to the zwitterionic polyaspartamide nanogel *N*_α-Lys-NG. In this case, loading of 1 and 0.75 mg/ml of the ¹²⁵I-radiolabeled BSA resulted in average loading capacities 11.1 % (11.1 µg/ml) and 14.8 % (11.1 µg/ml). As was observed in other works, the high loading efficiency 35.9 % (18 µg/ml) was found when *N*_α-Lys-NG was incubated with 0.5 mg/ml ¹²⁵I-radiolabeled BSA [31,33]. Interestingly, our results show that the amount of adsorbed ¹²⁵I-radiolabeled BSA increased with the decrease of initial concentration of the ¹²⁵I-radiolabeled BSA. The reverse effect was found with the loading of BSA onto poly(acrylic acid) and hybrid hydroxyapatite nanoparticles with chitosan/polyacrylic acid nanogels where the loading was predominantly influenced by electrostatic interaction [34,35]. Our observation indicates that the adsorption of ¹²⁵I-radiolabeled BSA onto *N*_α-Lys-NG is mainly driven by hydrophobic interaction, and at higher initial ¹²⁵I-radiolabeled BSA concentrations both polypeptide nanogels *N*_α-Lys-NG and PHEG-Tyr are quickly saturated and unable to adsorb higher amount of ¹²⁵I-radiolabeled BSA. The burst release of adsorbed BSA could be observed 1h after the beginning of the release study. This release behavior

continued up to 6h (Figure 4b) and was followed by the cumulative release over the next 162 h with a final release of ~ 65%. Clearly, some fraction of ^{125}I -radiolabeled BSA was again entrapped in the shrunken N_α -Lys-NG nanogel after the pH change (Figure 3a), probably due to high electrostatic interaction during the release at pH 7.4.

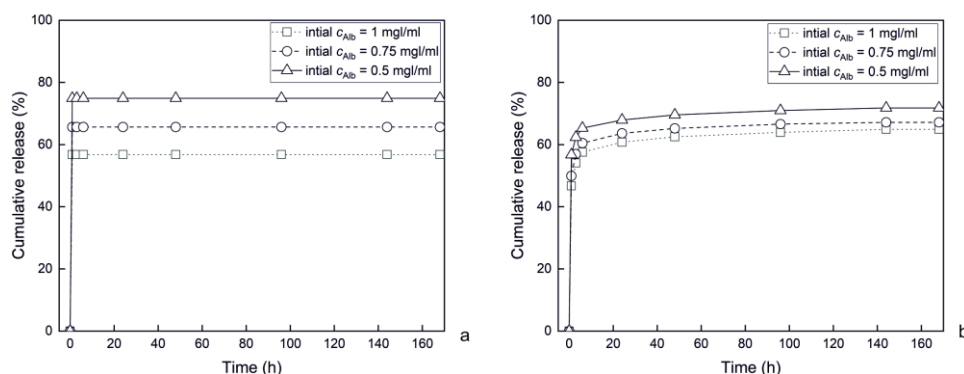


Figure 4. Release of ^{125}I -radiolabeled albumin from PHEG-Tyr (a) and N_α -Lys-NG (b) nanogels at initial ^{125}I -radiolabeled albumin concentration 1 (\square), 0.75 (\circ), and 0.5 mg/ml (Δ).

After the loading and release procedure was optimized with BSA, PHEG-Tyr and N_α -Lys-NG nanogels were incubated with three different concentrations of ^{125}I -radiolabeled AAT (1, 0.75 and 0.5 mg/ml) to investigate the loading capacity and release profiles. Due to the fact that AAT has pI in the range 4.2-4.9, we loaded AAT at pH 4.7 as it was optimized with BSA to ensure efficient adsorption of AAT [31,32]. PHEG-Tyr nanogel again adsorbed a low amount of ^{125}I -radiolabeled AAT (~4 %) documented by 42, 23, and 22 $\mu\text{g/ml}$ of loaded ^{125}I -radiolabeled AAT, respectively. The burst release profile was observed within 6 h and the release equilibrium was reached after 168h (Figure 5a). Approximately 35 % ^{125}I -radiolabeled AAT was retained in PHEG-Tyr nanogel after the release study at pH 7.4. Assumably, the ^{125}I -radiolabeled AAT was mainly adsorbed and released from the surface of the PHEG-Tyr nanogel while some fraction of the ^{125}I -radiolabeled AAT was trapped in the collapsed PHEG-Tyr nanogel after the pH change (Figure 2a). The loading and release study showed the same trend, namely that the released ^{125}I -radiolabeled AAT increased with decreased ^{125}I -radiolabeled AAT initial concentration. Clearly, higher ^{125}I -labeled AAT concentration leads to fast saturation of PHEG-

Tyr due to immediate interaction that hinders subsequent adsorption of the ^{125}I -radiolabeled AAT. In the case of N_{α} -Lys-NG nanogel, the amount of adsorbed ^{125}I -radiolabeled AAT increased from 11.9 (119 $\mu\text{g/ml}$, 14.2 (106 $\mu\text{g/ml}$) to 20 % (100 $\mu\text{g/ml}$) with the decrease of initial concentration of ^{125}I -radiolabeled AAT (1, 0.75, 0.5 mg/ml), followed by the same burst release, which was finished after 6 h and sustained release followed over the next 162 h (Figure 5b). The release profile was not affected by the initial concentration of ^{125}I -radiolabeled AAT. However, $\sim 40\%$ was of ^{125}I -radiolabeled AAT was captured in the N_{α} -Lys-NG nanogel after the release equilibrium was reached.

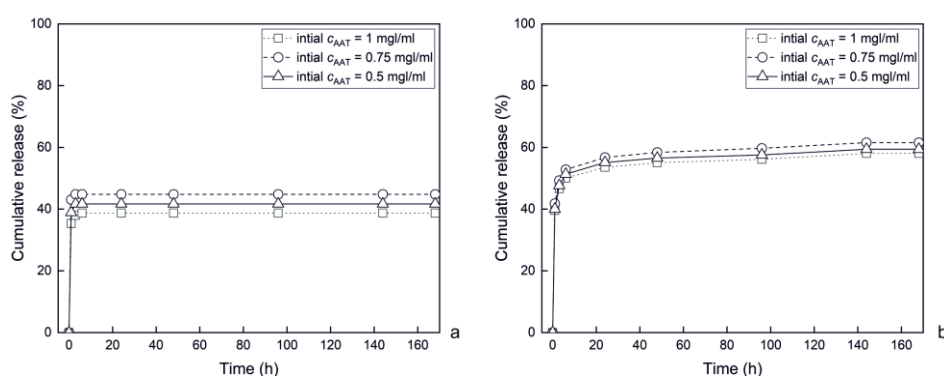


Figure 5. Release of ^{125}I -radiolabeled α -1-antitrypsin from PHEG-Tyr (a) and N_{α} -Lys-NG (b) nanogels at initial ^{125}I -radiolabeled α -1-antitrypsin concentration 1 (\square), 0.75 (\circ), and 0.5 mg/ml (Δ).

The loading and release study showed that the zwitterionic polyaspartamide N_{α} -Lys-NG nanogel exhibited better loading capacity for the ^{125}I -radiolabeled BSA as a model protein and ^{125}I -radiolabeled AAT in comparison to the PHEG-Tyr nanogel. Both nanogels demonstrated the burst release for over 6 h. Such release behavior of polypeptide nanogel with the loaded natural inhibitor AAT could be advantageous for prompt inhibition of the inflammatory mediator trypsin.

Pilot in vitro study of trypsin inhibition

Therefore, as a next step, inhibition activity of PHEG-Tyr and N_{α} -Lys-NG nanogels loaded with AAT was investigated by spectrophotometric measurement at $\lambda = 253\text{ nm}$ according to the modified procedure of enzymatic assay of trypsin. The trypsin inhibition study was carried out at two

trypsin:substrate ratios of 1:50 and 1:25. The trypsin:AAT ratio was 1:1 for both trypsin:substrate ratios. According to the previous loading studies of ^{125}I -radiolabeled ATT onto PHEG-Tyr and N_α -Lys-NG nanogels, the maximum loading capacities of AAT were found and the corresponding amount of PHEG-Tyr and N_α -Lys-NG nanogels were calculated. In each pilot trypsin inhibition activity of PHEG-Tyr nanogel loaded with AAT (\square), N_α -Lys-NG loaded with AAT (\circ), AAT (\diamond), and conversion of BAEE substrate with trypsin without inhibition (Δ) were tested.

At trypsin:substrate ratio 1:50, the maximum conversion of BAEE with trypsin without inhibition was reached during 15 min (Figure 6a; curve Δ). In presence of AAT inhibitor, the consumption of BAEE by trypsin was not affected by the presence of AAT due to the low concentration of the inhibitor which could not concur over the BAEE conversion (Figure 6a; curve \diamond). Next, we observed that the trypsin activity was slightly inhibited by N_α -Lys-NG loaded with AAT (Figure 6a; curve \circ), and the inhibition effect was more pronounced when biocompatible and biodegradable PHEG-Tyr nanogel loaded with AAT was used (Figure 6a; \square). For trypsin:substrate ratio 1:25, full conversion of BAEE with trypsin without inhibition was achieved within 3 minutes (Figure 6b; curve Δ). This trypsin:substrate ratio was found to be the most favorable for further inhibition studies. Clearly, AAT decreased the activity of trypsin only slightly (Figure 6b; curve \diamond), while increased inhibition was observed when AAT was loaded into both the tested nanogels. PHEG-Tyr nanogel (Figure 6a; \square) demonstrated better inhibition activity over N_α -Lys-NG nanogel (Figure 6b; curve \circ). Interestingly, this observation proves that the inhibition activity of ATT is reinforced by N_α -Lys-NG and even more by PHEG-Tyr, probably caused by their negative charge which facilitates positioning of ATT and blockage of the trypsin active site [8]. These results prove that the developed nanogel systems loaded with AAT can successfully block the active site of trypsin and inhibit its enzymatic activity during conversion BAEE substrate. This pilot *in vitro* study was crucial for the development of functional, fully biocompatible and biodegradable nanogel carrier that will serve for subsequent optimization of the inhibition effect of PHEG-Tyr nanogel loaded with AAT varying trypsin:substrate ratio, PHEG-Tyr and AAT amounts and finally for *in vivo* inhibition study with animal models.

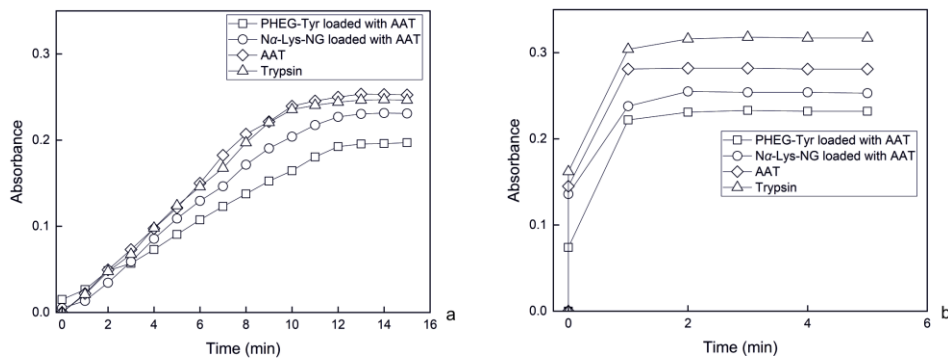


Figure 6. Spectrophotometric measurement of enzymatic assay of trypsin at trypsin:substrate ratio 1:50 (a) and 1:25 (b) using trypsin without inhibition (Δ), AAT (\diamond), N_{α} -Lys-NG loaded with AAT (o), and PHEG-Tyr nanogel loaded with AAT (\square).

Conclusions

In this study, newly developed hydrophilic, biocompatible, and biodegradable nanogel delivery systems of AAT based on polyglutamine PHEG-Tyr and polyaspartamide N_{α} -Lys-NG were prepared by HRP/ H_2O_2 -mediated crosslinking in inverse miniemulsion. Both negatively charged polypeptide nanogels demonstrated pH stimuli-responsive behavior and thermal transition documented by changed hydrodynamic diameters. The loading and release procedures with PHEG-Tyr and N_{α} -Lys-NG were firstly optimized with BSA and then AAT loading and release was studied. The results show that AAT has an affinity to both nanogels and the burst release of AAT during 6 h with following continuous release during ~ 160 h was observed. Finally, both nanogels were used as AAT depots for the inhibition of inflammatory mediator trypsin. The pilot *in vitro* enzymatic study proved the ability of the nanogels loaded with AAT to successfully inhibit trypsin. Moreover, both AAT-loaded nanogels have better inhibition activity in comparison to AAT itself. This indicates that the fully biocompatible nanogel systems might be potential candidates for the development of new inhibitory system of inflammatory mediator trypsin and possibly for the treatment of pancreatitis. Last but not least, this study will serve for future optimization of the new type inhibition nanogel system and subsequent *in vivo* experiments with animal models.

Experimental

Materials

Benzene p.a., cyclohexane p.a. (CHX), chloroform p.a., *N,N*-dimethylformamide p.a. (DMF), 1,4-dioxane p.a., methanol p.a., and tetrahydrofuran p.a. (THF) were obtained from Lach-Ner (Czech Republic). The solvents were purified and dried by a standard procedure before use. Aminopropan-2-ol (purified by vacuum distillation) was purchased from Alfa Aesar (Kandel, Germany). 1,6-Diaminohexane, HBr 33 wt% in acetic acid, 30% hydrogen peroxide solution (w/w) in water containing stabilizer (H₂O₂), horseradish peroxidase type VI (HRP), α_1 -antitrypsin from human plasma (AAT), trypsin from bovine pancreas type I, propargylamine, ethanolamine, *N* α -benzoyl-L-arginine ethyl ester hydrochloride (BAEE), *N* α -(tert-butoxycarbonyl)-L-lysine (Boc-Lys-OH), polyoxyethylenesorbitan trioleate (TWEEN 85), sodium methoxide, sorbitan monooleate (SPAN 80), triphosgene, and tyramine were purchased from Sigma-Aldrich (Prague, Czech Republic) and were used without purification. γ -Benzyl-L-glutamate (BLG) 99% was purchased from Emmenar Bio-Tech (Sanathnagar, India) and was recrystallized from a hot water/ethanol mixture. OxymaPure was purchased from Irish Biotech (Marktredwitz, Germany). PD-10 desalting columns (Sephadex G 25) were obtained from Amersham Biosciences (Uppsala, Sweden). Na¹²⁵I-radiolabeling solution (3 700 MBq/ml) was purchased from the Institute of Isotopes (Budapest, Hungary). The Pierce™ Iodination Beads were received from Thermo Fisher Scientific.

Preparation of polyglutamine (PHEG-Tyr) and zwitterionic polyaspartamide (N α -Lys-NG) nanogels

The PHEG-Tyr polymer precursor containing 10.8 wt% of Tyr units was prepared and characterized according to a previously published procedure [23]. PHEG-Tyr nanogel was prepared by HRP/H₂O₂-mediated crosslinking in inverse miniemulsion by modification of an earlier procedure [24]. Briefly, PHEG-Tyr (0.18 g) was dissolved in Q-H₂O (4 g) in a round-bottom glass flask for 24 h at room temperature under magnetic stirring. Then, HRP (0.450 mg) was dissolved in Q-H₂O (0.32 g) and added to the PHEG-Tyr aqueous solution. The surfactants SPAN 80 (0.855 g) and TWEEN 85 (0.045 g) were dissolved in CHX (20.4 g) and mixed with the aqueous solution of PHEG-Tyr with HRP. This two-

phase system was cooled to 0 °C and dispersed using a UP200Ht ultrasonic processor equipped with a sonotrode S26d7 (Hielscher Ultrasonics GmbH, Teltow, Germany) for 150 s at an amplitude of 40%. The formed inverse miniemulsion was transferred into a 30-mL glass reaction vessel equipped with an anchor-type stirrer (500 rpm). Finally, H₂O₂ (16 μL) was added with a syringe, and the nanogelation run at room temperature for 2 h. The nanogel was separated by centrifugation (11,000 rpm/20 min), washed three times with CHX, dispersed in CHX (20 mL) overnight, and again washed seven times with CHX to completely remove any residual surfactant. Then, the nanogel was dispersed in distilled water and dialyzed (molecular weight cut-off < 100 kDa) against distilled water for 7 days. Finally, the nanogel was freeze-dried from distilled water.

The zwitterionic polyaspartamide nanogel (*N*_α-Lys-NG) was prepared by the indirect strategy from polyaspartamide with protected zwitterionic groups (*N*_α-Lys-P-HE-TyrAA) with the following deprotection step leading to the formation of nanogel with zwitterionic groups according to our earlier published procedure [25].

Characterization of nanogels

The DLS and zeta potential measurements were performed with dispersions of PHEG-Tyr and *N*_α-Lys-NG nanogels in PBS buffer at pH 4, 4.5, 4.7, 5.5, and 7.4 (1 mg/ml) at 25 and 37 °C using Zetasizer Nano ZS (Malvern Instruments Ltd., Worcestershire, UK) at 633 nm and 173° detection angle. Size and size distribution were obtained from the correlation function using CONTIN analysis available in the Malvern software. The hydrodynamic diameters (*D*_H) were calculated using the Stokes-Einstein equation. For DLS measurements, both nanogels were dispersed in Q-H₂O (2 mL; 1 mg/mL) in glass vials by a UP200Ht ultrasonic processor equipped with sonotrode S26d2 for 5 min at 40% amplitude using the following method: 2 min with pulsation (0.5 s pulse rate), 2 min without pulsation, and 1 min with pulsation (0.5 s pulse rate).

The nanogel morphology, size and particle size distribution were studied using a Tecnai G2 Spirit Twin 12 transmission electron microscope (TEM; FEI; Brno, Czech Republic) after negative staining of nanogel samples with uranyl acetate. The number-average diameter (*D*_n), weight-average

diameter (D_w), and dispersity (\mathcal{D}) were calculated using ImageJ software by counting the hydrogel nanoparticles in the TEM images following these equations:

$$D_n = \frac{\sum n_i D_i}{\sum n_i} \quad (1),$$

$$D_w = \frac{\sum n_i D_i^4}{\sum n_i D_i^3} \quad (2),$$

$$\mathcal{D} = \frac{D_w}{D_n} \quad (3),$$

where n_i and D_i are the number and diameter of the i -th microsphere, respectively.

¹²⁵I-radiolabeling, loading and release of bovine serum albumin (BSA) and α -1-antitrypsin (AAT)

Solution of BSA (10 mg), or AAT (10 mg), in PBS buffer (400 μ l, pH 7.4) was reacted with [¹²⁵I]-NaI solution (155 MBq) for 30 min in a presence of two IODO-BEADS (pre-washed with PBS buffer, pH 7.4). After the separation of IODO-BEADS, a solution of ascorbic acid (10 μ l, 25 mg/ml in PBS buffer, pH 7.4) was added to the ¹²⁵I-radiolabeled BSA, or ¹²⁵I-radiolabeled AAT, and incubated for 30 min. Finally, the ¹²⁵I-radiolabeled BSA, or ¹²⁵I-radiolabeled AAT, was separated with a PD10 desalting column to remove impurities, unreacted compounds, and low molecular fractions. The purified fraction of the ¹²⁵I-radiolabeled BSA, or ¹²⁵I-radiolabeled AAT, was used in the following experiments.

PHEG-Tyr nanogel dispersion (0.5 ml, 3 mg/ml in PBS buffer with pH 4.7) was mixed with the solution ¹²⁵I-radiolabeled BSA (0.5 ml), or ¹²⁵I-radiolabeled AAT (0.5 ml), in PBS buffer (pH 7.4) to obtain solutions with three different BSA concentrations 1, 0.75, and 0.5 mg/ml in separate microtubes. pH of the loading assays was adjusted to pH 4.7 with the addition of 5 μ l of 1 M HCl. The final concentration of PHEG-Tyr nanogel in the loading assays was 1.5 mg/ml. The loading of ¹²⁵I-radiolabeled BSA, or ¹²⁵I-radiolabeled AAT, was performed for 24 h at 25 °C under mild shaking. Then, the loading assays were centrifuged (7,000 rpm/10 min). Supernatants were removed with a micropipette and placed in clear microtubes. The radioactivity of PHEG-Tyr nanogels and supernatants was measured using a 2480 Wizard2® Automatic Gamma Counter (PerkinElmer, Massachusetts, USA) to determine a loading capacity of PHEG-Tyr nanogel.

PHEG-Tyr nanogels loaded with ¹²⁵I-radiolabeled BSA, or ¹²⁵I-radiolabeled AAT, were redispersed in fresh PBS buffer (0.5 ml) to study a release profile 25 °C. In exact time intervals ($t = 1$,

3, 6, 24, 48, 96, 144, and 168 h), the PHEG-Tyr nanogel was removed by centrifugation (7,000 rpm/10 min) and radioactivity of the supernatant with released ^{125}I -radiolabeled BSA, or ^{125}I -radiolabeled AAT, and the radioactivity of PHEG-Tyr nanogel pellet loaded with ^{125}I -radiolabeled BSA, or ^{125}I -radiolabeled AAT, were measured using a 2480 Wizard2® Automatic Gamma Counter. Then, the PHEG-Tyr nanogel was redispersed in fresh PBS buffer (0.5 ml, pH 7.4) to continue the release study.

Loading of ^{125}I -radiolabeled BSA, or ^{125}I -radiolabeled AAT using N_α -Lys-NG nanogel was performed according to the same procedure.

All measurements were made in triplicate and averaged.

Spectrophotometric measurement of inhibition of trypsin enzymatic activity

Inhibition assay carried out at trypsin:substrate molar ratio 1:50 and 1:25. Trypsin:AAT molar ratio was 1:1. Firstly, PHEG-Tyr (6.97 mg and 3.48 mg), or N_α -Lys-NG (1.53 mg and 0.77 mg) were dispersed in PBS (4.5 ml, pH 4.7) and loaded with AAT (0.102 and 0.051 mg) for 24 h, respectively. The assay was prepared by mixing of BAEE solution (2 ml, 0.37 mM) in PBS buffer (pH 7.6) with 1mM HCl (0.125 ml), dispersion of AAT loaded-PHEG-Tyr, or AAT loaded- N_α -Lys-NG, nanogel (1 ml), and trypsin solution (0.075 ml) in 1mM HCl in cuvettes for UV-Vis spectrophotometric measurement. Immediately after the mixing, the absorbance at $\lambda = 253$ nm was recorded for 5 or 15 mins using 1 min time period at 25 °C. A blank solution was prepared by mixing N_α -benzoyl-L-arginine ethyl ester substrate solution (2 ml, 0.375 mM) in PBS buffer (pH 7.6) with 1mM HCl (0.125 ml), and dispersion of AAT loaded-PHEG-Tyr, or AAT loaded- N_α -Lys-NG, nanogel (1 ml). Inhibition assay using only AAT without the nanogels was prepared by solving AAT (0.102 and 0.051 mg) in PBS buffer (4 ml, pH 4.7) following the same procedure. Trypsin enzymatic assay was prepared by mixing BAEE solution (3 ml, 0.375 mM) in PBS buffer (pH 7.6) with 1mM HCl (0.125 ml) and relevant trypsin solution (0.075 ml) in 1mM HCl in cuvettes for UV-Vis spectrophotometric measurement. Immediately after mixing, the absorbance at $\lambda = 253$ nm was recorded for 5 or 15 mins using 1 min time period. The blank solutions were prepared without the addition of trypsin and with 0.2 ml 1 mM HCl. All measurements were made in triplicate and averaged.

Funding: Financial support from the Czech Science Foundation (No. 21-06524S) and from Ministry of Education, Youth and Sports of the Czech Republic (grant # EATRIS-CZ LM2018133 ERIC) are gratefully acknowledged.

Conflicts of Interest: The authors declare no conflict of interest.

References

1. Ouyang, G.; Pan, G.; Liu, Q.; Wu, Y.; Liu, Z.; Lu, W.; Li, S.; Zhou, Z.; Wen, Y. *BMC Med.* **2020**, *18*, 388.
2. Drake, M.; Dodwad, S. J. M.; Davis, J.; Kao, L. S.; Cao, Y.; Ko, T. C. *J. Clin. Med.* **2021**, *10*, 300.
3. Xiao, A. Y.; Tan, M. L. Y.; Wu, L. M.; Asrani, V. M.; Windsor, J. A.; Yadav, D.; Petrov, M. S. *Lancet Gastroenterol. Hepatol.* **2016**, *1*, 45-55.
4. Szabó A., Toldi V., Gazda L. D., Demcsák A., Tözsér J., Sahin-Tóth M. *J. Biol. Chem.* **2021**, *296*, 100343.
5. Gui, F.; Zhang, Y.; Wan, J.; Zhan, X.; Yao, Y.; Li, Y.; Haddock, A. N.; Shi, J.; Guo, J.; Chen, J.; Zhu, X.; Edenfield, B. H.; Zhuang, L.; Hu, C.; Wang, Y.; Mukhopadhyay, D.; Radisky, E. S.; Zhang, L.; Lugea, A.; Pandol, S. J.; Bi, Y.; Ji, B. *J. Clin. Invest.* **2020**, *130*, 189-202.
6. Brandl, T.; Simic, O.; Skaanderup, P. R.; Namoto, K.; Berst, F.; Ehrhardt, C.; Schiering, N.; Mueller, I.; Woelcke, J. *Bioorganic Med. Chem. Lett.* **2016**, *26*, 4340-4344.
7. Liu, K. *J. Am. Oil Chem. Soc.* **2021**, *98*, 355-373.
8. Pouvreau, L.; Chobert, J. M.; Briand, L.; Quillien, L.; Tran, V.; Guéguen, J.; Haertlé, T. *FEBS Lett.* **1998**, *423*, 167-172.
9. Chanphai, P.; Tajmir-Riahi, H. A. *Carbohydr. Polym.* **2016**, *144*, 346-352.
10. Mao, X.; Yang, Z. *Ann. Palliat. Med.* **2021**, *10*, 1325-1335.
11. Beghdadi, W.; Madjene, L. C.; Benhamou, M.; Charles, N.; Gautier, N.; Launay, P.; Blank, U. *Front. Immunol.* **2011**, *2*, 37.
12. Hashimoto, Y.; Mukai, S. A.; Sasaki, Y.; Akiyoshi, K. *Adv. Healthc. Mater.* **2018**, *7*, 1800729.

13. Vashist, A.; Kaushik, A.; Vashist, A.; Bala, J.; Nikkhah-Moshaie, R.; Sagar, V.; Nair, M. *Drug Discov. Today* **2018**, *23*, 1436-1443.
14. Massi, L.; Najer, A.; Chapman, R.; Spicer, C. D.; Nele, V.; Che, J.; Booth, M. A.; Douth, J. J.; Stevens, M. M. *J. Mater. Chem. B* **2020**, *8*, 8894-8907.
15. Ozawa, Y.; Sawada, S. I.; Morimoto, N.; Akiyoshi, K. *Macromol. Biosci.* **2009**, *9*, 694-701.
16. Hirakura, T.; Yasugi, K.; Nemoto, T.; Sato, M.; Shimoboji, T.; Aso, Y.; Morimoto, N.; Akiyoshi, K. *J. Control. Release* **2010**, *142*, 483-489.
17. Morimoto, N.; Hirano, S.; Takahashi, H.; Loethen, S.; Thompson, D. H.; Akiyoshi, K. *Biomacromolecules* **2013**, *14*, 56-63.
18. Alkanawati, S. M.; Machtakova, M.; Landfester, K.; Thérien-Aubin, H. *Biomacromolecules* **2021**, *22*, 2976-2984.
19. Dunlea, D. M.; Fee, L. T.; McEnery, T.; McElvaney, N. G.; Reeves, E. P. *J. Inflamm. Res.* **2018**, *11*, 123-134.
20. Stockley, R. A. *Ann. Transl. Med.* **2015**, *3*, 130.
21. Pirooznia, N.; Hasannia, S.; Lotfi, A. S.; Ghanei, M. *J. Nanobiotechnology* **2012**, *10*, 20.
22. Arjmand, S.; Bidram, E.; Lotfi, A. S.; Mahdavi, H.; Alavi, M. *Int. J. Biosci. Biochem. Bioinform.* **2011**, *1*, 68-72.
23. Dvořáková, J.; Šálek, P.; Korecká, L.; Pavlova, E.; Černocho, P.; Janoušková, O.; Koutníková, B.; Proks, V. *J. Appl. Polym. Sci.* **2020**, *137*, 48725.
24. Oleshchuk, D.; Šálek, P.; Dvořáková, J.; Kučka, J.; Pavlova, E.; Francová, P.; Šefc, L.; Proks, V. *Mater. Sci. Eng. C* **2021**, *126*, 111865.
25. Hladys, S.; Oleshchuk, D.; Dvořáková, J.; Golunova, A.; Šálek, P.; Pánek, J.; Janoušková, O.; Kaňková, D.; Pavlova, E.; Proks, V. *Eur. Polym. J.* **2021**, *148*, 110347.
26. Marciel, A. B.; Chung, E. J.; Brettmann, B. K.; Leon, L. *Adv. Colloid Interface Sci.* **2017**, *239*, 187-198.
27. Pujana, M. A.; Pérez-Álvarez, L.; Iturbe, L. C. C.; Katime, I. *Eur. Polym. J.* **2014**, *61*, 215-225.
28. Bordat, A.; Boissenot, T.; Nicolas, J.; Tsapis, N. *Adv. Drug Deliv. Rev.* **2019**, *138*, 167-192.
29. Ostolska, I.; Wiśniewska, M. *Colloid Polym. Sci.* **2014**, *292*, 2453-2464.

30. Argentiere, S.; Blasi, L.; Ciccarella, G.; Barbarella, G.; Cingolani, R.; Gigli, G. *J. Appl. Polym. Sci.* **2010**, *116*, 2808-2815.
310. Zhang, Y.; Zhang, D.; Wang, J. T.; Zhang, X.; Yang, Y. *Polym. Chemistry* **2021**, *12*, 554. DOI: 10.1039/D0PY01600D
32. Wang, Q.; Xu, H.; Yang, X.; Yang, Y. *Int. J. Pharm.* **2008**, *361*, 189-193.
33. Lale, S. V.; Koul, V. Stimuli-Responsive Polymeric Nanoparticles for Cancer Therapy In *Polymer Gels Prospectives and Applications*, Thakur, V. K., Thakur, M. K., Voicu, S. I., Eds.; Springer, Singapore., 2018; pp. 27-54.
34. Chen, Y.; Zheng, X.; Qian, H.; Mao, Z.; Ding, D.; Jiang, X. *ACS Appl. Mater. Interfaces* **2010**, *2*, 3532-3538.
35. Qin, J.; Zhong, Z.; Ma, J. *Mater. Sci. Eng. C* **2016**, *62*, 377-383.